

Energy Spectra from Electromagnetic Fields Generated by Ultra-relativistic Charged Bunches in a Perfectly Conducting Cylindrical Beam Pipe

Alison C Hale* and Robin W Tucker†

Department of Physics, Lancaster University

and the Cockcroft Institute,

Keckwick Lane,

Daresbury, WA4 4AD, UK

November 8, 2009

Abstract

The spectrum of electromagnetic fields satisfying perfectly conducting boundary conditions in a segment of a straight beam pipe with a circular cross-section is discussed as a function of various source models. These include charged bunches that move along the axis of the pipe with constant speed for which an exact solution to the initial-boundary value problem for Maxwell's equations in the beam pipe is derived. In the ultra-relativistic limit all longitudinal components of the fields tend to zero and the spectral content of the transverse fields and average total electromagnetic energy crossing any section of the beam pipe are directly related to certain properties of the ultra-relativistic source. It is shown that for axially symmetric ultra-relativistic bunches interference effects occur analogous to those that occur due to CSR in cyclic machines despite the fact that in this limit the source is not accelerating. The results offer an analytic description of the fields showing how enhanced spectral behaviour depends on the geometry of the source, its location in the beam pipe and the details of the stochastic distribution of the source structure. The results are illustrated for different situations associated with the motion of on-axis ultra-relativistic bunches. The field energy spectra associated with a source containing \mathcal{N} identically charged ultra-relativistic pulses, each with individual longitudinal gaussian profiles distributed according to a uniform probability distribution with compact support, is compared with that generated by charged bunches containing a distribution with $2n + 1$ peaks in a region with compact support (modeling micro-bunches). These results are of relevance for the experimental determination of properties of the longitudinal charge distribution of short relativistic electron bunches with micro-structure in straight segments of a beam pipe, from observation of the associated electromagnetic energy spectra.

*a.c.hale@lancaster.ac.uk

†r.tucker@lancaster.ac.uk

1 Introduction

Modeling the behaviour of charged particles in a modern accelerator is a critical component in its design. Due to the inherent non-linear nature of the dynamics of charged bunches in external electromagnetic fields such modeling generally necessitates numerical computation. With current hardware such computations often require further stringent approximations on the equations of motion in order to extract viable information. To date the most sophisticated Maxwell-Vlasov solvers are unable to effectively model electromagnetic interference in 3 spatial dimensions. Approximations often neglect the effects of confining boundaries and wakes, radiation reaction forces, detailed stochastic properties of the beam and possible quantum effects. However, in certain limits *analytic* information can be deduced from the fundamental equations of motion for the coupled particle field system. If the motion is prescribed the problem reduces to solving Maxwell's equations for convected sources. Nevertheless finding solutions satisfying boundary condition appropriate to an accelerator is in general a non-trivial exercise.

Since Fourier analysis is a linear operation the spectral content of the electromagnetic energy in the fields produced by charged particles in prescribed motion *in free space* has been exhaustively investigated over many decades, particularly for collections of particles in uniform circular motion [1, 2]. The effects of the superposition of retarded free-space solutions to Maxwell's equations with distributed currents on the spectral content of their radiation fields gave rise to the notion of *coherent synchrotron radiation* (CSR) in which enhanced radiation in some frequency domain can occur, depending quadratically on the total number of point particles in an accelerating bunch [3]. In a synchrotron CSR criteria are generally inferred from the motion of collections of charged particles distributed on segments of a circular arc and interference associated with the phases of the *radiation components* of the fields. It is generally assumed that the effects of confining boundaries in a such a machine do not significantly alter the *criteria* for CSR from those that arise for relativistic sources in free space. However analytic efforts to determine such criteria taking account of boundary conditions and stochastic effects inevitably demand further approximations [4, 5]. In general the presence of boundaries introduces additional scales into the problem of calculating the electromagnetic fields produced by the sources. The manner in which such scales affect the subsequent criteria for coherence depends on solving Maxwell's equations subject to the appropriate boundary conditions. Since the role of CSR is a fundamental ingredient in the design of new light sources and a general knowledge of the spectral content of the fields produced by ultra-relativistic bunches is important for the operation new electro-optic diagnostic tools [6] it is of interest to explore new analytic approximations schemes that can complement the numerical simulations of particle-field interactions.

In this note we consider solving Maxwell's equations for model sources in a straight beam pipe. By exploiting the properties of particular mode functions we ensure at the outset that all fields satisfy perfectly conducting boundary conditions in a straight beam pipe with a circular cross-section and an exact solution to the initial-boundary value problem for Maxwell's equations in the beam pipe is derived. Although in principle our approach

can accommodate sources in arbitrary motion attention will be restricted to those that move along the axis of the pipe with constant speed. In conventional terminology the fields associated with such sources are “bound” rather than “radiative”. In the ultra-relativistic limit all longitudinal components of the fields tend to zero and the spectral content of the transverse fields and average total electromagnetic energy crossing any section of the beam pipe are directly related to the properties of the ultra-relativistic source. Thus a measurement of the former offers a direct method of estimating properties of the latter. However the detailed structure of the spectral content depends on the source structure. In particular we demonstrate that for bunches with axially symmetric charge distributions in ultra-relativistic motion along the pipe axis interference effects occur with properties that are analogous to those that occur due to CSR in cyclic machines, despite the fact that in this limit the source is not accelerating. Furthermore it is possible to study analytically how such enhanced spectral behaviour depends on the geometry of the source, the radius of the beam pipe and details of the stochastic distribution of structure within the source.

Section 2 establishes the formalism for solving Maxwell’s equations for fields inside a perfectly conducting cylindrical beam pipe in terms of complex Dirichlet and Neumann eigen-modes of the 2-dimensional scalar Laplacian operator. An exact solution to the initial-boundary value problem is exhibited and this is used to explore fields associated with ultra-relativistic bunches. Section 3 develops the model in terms of an axially symmetric ultra-relativistic source and offers a compact formula for the spectral distribution of electromagnetic energy that crosses any section of the beam. Section 4 discusses the effects on the spectra produced by different types of stochastic source distribution.

2 Electromagnetic Field Solutions

The electromagnetic fields \mathbf{e} and \mathbf{h} in a beam pipe in the presence of sources with charge density ρ and electric current density \mathbf{J} satisfy the Maxwell system:

$$\nabla \times \mathbf{e} + \mu_0 \partial_t \mathbf{h} = 0 \quad (1)$$

$$\nabla \times \mathbf{h} - \mu_0 Y^2 \partial_t \mathbf{e} - \mathbf{J} = 0 \quad (2)$$

$$\nabla \cdot \mathbf{h} = 0 \quad (3)$$

$$\mu_0 Y^2 \nabla \cdot \mathbf{e} - \rho = 0 \quad (4)$$

where the admittance $Y = 1/(\mu_0 c)$ with c being the speed of light in vacuo. All vectors will be referred to a local ortho-normal frame $\{\hat{\mathbf{e}}_r, \hat{\mathbf{e}}_z, \hat{\mathbf{e}}_\theta\}$ defining a cylindrical coordinate system $\{r, \theta, z\}$ with the axis of the beam pipe along the z -axis.

A transverse circular section of this pipe of radius a is denoted \mathcal{D} with boundary $\partial\mathcal{D}$. In the following we exploit the properties of a *complex Dirichlet mode set* $\{\Phi_N\}$. This is a collection of complex eigen-functions of the 2-dimensional (transverse) Laplacian operator $\hat{\Delta}$ on \mathcal{D} that vanishes on $\partial\mathcal{D}$. This boundary condition determines the associated (positive non-zero real) eigenvalues β_N^2 . The label N here consists of an ordered pair of real numbers. Thus

$$\hat{\Delta}\Phi_N - \beta_N^2\Phi_N = 0, \quad (5)$$

with $\Phi_N|_{\partial\mathcal{D}} = 0$ and

$$\hat{\Delta} = -\frac{1}{r} \frac{\partial}{\partial r} \left(r \frac{\partial}{\partial r} \right) - \frac{1}{r^2} \frac{\partial^2}{\partial \theta^2} \quad (6)$$

With an overbar indicating complex conjugation these modes are normalised to satisfy

$$\int_{\mathcal{D}} \overline{\Phi_M} \Phi_N r dr d\theta = \mathcal{N}_N^2 \delta_{NM}, \quad (7)$$

An explicit form for Φ_N is for $n \in \mathbb{Z}$

$$\Phi_N(r, \theta) = J_n \left(x_{q(n)} \frac{r}{a} \right) e^{in\theta}, \quad (8)$$

where $J_n(x)$ is the n -th order Bessel function and the numbers $\{x_{q(n)}\}$ are defined by $J_n(x_{q(n)}) = 0$ and $N := \{n, q(n)\}$. The eigenvalues are given by $\{\beta_N = x_{q(n)}/a\}$ and $\mathcal{N}_N^2 = \pi a^2 J_{n+1}^2(x_{q(n)})$.

In a similar manner a *Neumann mode set* $\{\Psi_N\}$ is a collection of eigen-functions of the Laplacian operator $\hat{\Delta}$ on \mathcal{D} such that $\frac{\partial\Psi_N}{\partial r}$ vanishes on $\partial\mathcal{D}$. This alternative boundary condition determines the associated (positive non-zero real) eigenvalues α_N^2 where again the label N consists of an ordered pair of real numbers:

$$\hat{\Delta}\Psi_N - \alpha_N^2\Psi_N = 0, \quad (9)$$

with $\frac{\partial\Psi_N}{\partial r}|_{\partial\mathcal{D}} = 0$. These modes are normalized to satisfy

$$\int_{\mathcal{D}} \overline{\Psi_M} \Psi_N r dr d\theta = \mathcal{M}_N^2 \delta_{NM}. \quad (10)$$

An explicit form for Ψ_M is for $m \in \mathbb{Z}$

$$\Psi_M(r, \theta) = J_m \left(x'_{p(m)} \frac{r}{a} \right) e^{im\theta}, \quad (11)$$

where the numbers $\{x'_{p(m)}\}$ are defined by $J'_m(x'_{p(m)}) = 0$ and $M := \{m, p(m)\}$. The eigenvalues are given by $\{\alpha_M = x'_{p(m)}/a\}$ and $\mathcal{M}_M^2 = \pi a^2 J_{m+1}^2(x'_{p(m)})$.

The electromagnetic fields in the interior of the cylindrical beam pipe satisfying perfectly conducting boundary conditions at $r = a$ can now be expanded [7, 8, 9] as:

$$\mathbf{e}(t, z, r, \theta) = \sum_N V_N^E(t, z) \nabla \Phi_N(r, \theta) + \sum_M V_M^H(t, z) \hat{\mathbf{e}}_z \times \nabla \Psi_M(r, \theta) + \sum_N \gamma_N^E(t, z) \Phi_N(r, \theta) \hat{\mathbf{e}}_z \quad (12)$$

$$\mathbf{h}(t, z, r, \theta) = \sum_N I_N^E(t, z) \hat{\mathbf{e}}_z \times \nabla \Phi_N(r, \theta) + \sum_M I_M^H(t, z) \nabla \Psi_M(r, \theta) + \sum_M \gamma_M^H(t, z) \Psi_M(r, \theta) \hat{\mathbf{e}}_z \quad (13)$$

The fields are assumed to be generated by an external RF source that accelerates charged bunches to near the speed of light. In a straight beam pipe such a source can be modeled by an arbitrary smooth *convective* charge density ρ and a current with ortho-normal components $J_r = J_\theta = 0$, $J_z(z - vt, r, \theta) = v \rho(z - vt, r, \theta)$ with constant v close to the speed of light. The equations for γ_N^H and γ_N^E that follow from Maxwell's equations and (12), (13) for these sources are:

$$\ddot{\gamma}_N^H - c^2 \gamma_N^{H''} + c^2 \alpha_N^2 \gamma_N^H = 0 \quad (14)$$

$$\ddot{\gamma}_N^E - c^2 \gamma_N^{E''} + c^2 \beta_N^2 \gamma_N^E = -\frac{c^2 \mu_0}{\mathcal{N}_N^2} (c^2 - v^2) \overline{\rho}_N \quad (15)$$

where

$$\rho_N := \int_{\mathcal{D}} \rho \Phi_N r dr d\theta. \quad (16)$$

In terms of γ_N^H and γ_N^E and the projected convective sources

$$V_N^E = \frac{1}{\beta_N^2} \left(\gamma_N^{E'} - \frac{1}{\mathcal{N}_N^2 \mu_0 Y^2} \overline{\rho}_N \right), \quad (17)$$

$$V_N^H = \frac{\mu_0}{\alpha_N^2} \dot{\gamma}_N^H, \quad (18)$$

$$I_N^E = -\frac{1}{\beta_N^2} \left(\mu_0 Y^2 \dot{\gamma}_N^E + \frac{v}{\mathcal{N}_N^2} \overline{\rho}_N \right), \quad (19)$$

$$I_N^H = \frac{1}{\alpha_N^2} \gamma_N^{H'}. \quad (20)$$

Finding the fields \mathbf{e} and \mathbf{h} is now reduced to solving an initial-value problem for the decoupled fields γ_N^H, γ_N^E . For some real constant $\sigma > 0$ and source $g(t, z)$ each is a solution to the generic (hyperbolic) partial differential equation

$$\ddot{f} - c^2 f'' + c^2 \sigma^2 f = g. \quad (21)$$

The general causal solution $f(t, z)$ with prescribed values of $f(0, z)$ and $\dot{f}(0, z)$, is (see e.g. [10])

$$f(t, z) = \mathcal{H}_\sigma[f^{init}](t, z) + \mathcal{I}_\sigma[g](t, z), \quad (22)$$

where

$$\begin{aligned}
\mathcal{H}_\sigma[f^{init}](t, z) &:= \frac{1}{2} \left\{ f(0, z - ct) + f(0, z + ct) \right\} \\
&+ \frac{1}{2c} \int_{z-ct}^{z+ct} d\zeta \dot{f}(0, \zeta) J_0(\sigma \sqrt{c^2 t^2 - (z - \zeta)^2}) \\
&- \frac{ct\sigma}{2} \int_{z-ct}^{z+ct} d\zeta f(0, \zeta) \frac{J_1(\sigma \sqrt{c^2 t^2 - (z - \zeta)^2})}{\sqrt{c^2 t^2 - (z - \zeta)^2}},
\end{aligned} \tag{23}$$

and

$$\mathcal{I}_\sigma[g](t, z) := \frac{1}{2c} \int_0^t dt' \int_{z-c(t-t')}^{z+c(t-t')} d\zeta g(t', \zeta) J_0(\sigma \sqrt{c^2(t-t')^2 - (z - \zeta)^2}), \tag{24}$$

The functions $f(0, z)$, $\dot{f}(0, z)$ constitute the initial $t = 0$ Cauchy data in this solution and determine the \mathcal{H}_σ contribution above.

For a bunch with total charge Q moving with speed v we assume here that ρ can be written

$$\rho(z - vt, r, \theta) = Q \rho^\perp(r, \theta) \rho^\parallel(z - vt), \tag{25}$$

where v is given ($v \leq c$) and $\rho^\perp(r, \theta)$, $\rho^\parallel(z - vt)$ are arbitrary smooth functions subject to

$$\int_{\mathcal{D}} \rho^\perp(r, \theta) r dr d\theta = 1, \quad \int_{-\infty}^{\infty} dz \rho^\parallel(z - vt) = 1, \tag{26}$$

With these sources the causal solutions to (14) and (15) for γ_N^H and γ_N^E are given by:

$$\begin{aligned}
\gamma_N^H(t, z) &= \mathcal{H}_{\alpha_N}[\gamma_N^{Hinit}](t, z), \\
\gamma_N^E(t, z) &= \mathcal{H}_{\beta_N}[\gamma_N^{Einit}](t, z) - \frac{\mu_0 c^2}{\mathcal{N}_N^2} (c^2 - v^2) \mathcal{I}_{\beta_N}[\overline{\rho'_N}](t, z),
\end{aligned} \tag{27}$$

where ρ_N is given by (16) and

$$\rho'_N(t, z) = Q \rho^{\parallel\prime}(z - vt) \int_{\mathcal{D}} \rho^\perp(r, \theta) \Phi_N r dr d\theta. \tag{28}$$

It is worth stressing that given the source (25) equations (27) and (28) provide analytic expressions from which the fields (12) and (13) can be constructed as mode sums. From these one can construct electromagnetic power flow from the Poynting vector and its Fourier transform using well established numerical techniques. In the ultra-relativistic limit, $v \rightarrow c$, the second term in $\gamma_N^E(t, z)$ tends to zero and for on-axis sources this offers a route to further analytic reduction in the next section.

3 Spectral Energy Distributions

When the transverse distribution depends only on r , expressions for the electromagnetic fields associated with the sources simplify. The source under consideration is axially symmetric if

$$\rho^\perp(r, \theta) = \mathcal{R}(r), \quad (29)$$

where $\mathcal{R}(r)$ is a smooth function satisfying

$$\int_0^a dr r \mathcal{R}(r) = \frac{1}{2\pi}. \quad (30)$$

Then for axially symmetric bunches

$$\rho'_N(t, z) = 2\pi Q_{tot} \delta_{n,0} \rho^{\parallel'}(z - vt) \int_0^a dr r \mathcal{R}(r) J_0\left(x_{q(0)} \frac{r}{a}\right). \quad (31)$$

From these formulae the instantaneous *real* electromagnetic power crossing any section of the beam pipe is obtained by integrating the component $S = (\mathbf{e} \times \mathbf{h}) \cdot \mathbf{e}_z$ of the Poynting vector field over the cross-section \mathcal{D} at an arbitrary point with coordinate z

$$\mathcal{P}(t, z) := \int_{\mathcal{D}} S(t, z, r, \theta) r dr d\theta \quad (32)$$

With the aid of the orthogonality properties of the Dirichlet and Neumann modes this becomes

$$\mathcal{P} = \Re \left\{ \sum_N \beta_N^2 \mathcal{N}_N^2 V_N^E \overline{I_N^E} - \sum_M \alpha_M^2 \mathcal{M}_M^2 V_M^H \overline{I_M^H} \right\}, \quad (33)$$

where \Re takes the real part of its argument. From (33), (17), (18), (19), and (20) this power flux can be explicitly expressed in terms of the source projections ρ_N and the field projections γ_M^H and γ_N^E

$$\begin{aligned} \mathcal{P} = & \Re \left\{ \sum_N \left(\frac{v |\rho_N|^2}{\mathcal{N}_N^2 \beta_N^2 \mu_0 Y^2} + \frac{\dot{\gamma}_N^E}{\beta_N^2} \rho_N - \frac{v \gamma_N^{E'}}{\beta_N^2} \rho_N \right. \right. \\ & \left. \left. - \frac{\mu_0 Y^2}{\beta_N^2} \mathcal{N}_N^2 \gamma_N^{E'} \overline{\dot{\gamma}_N^E} \right) - \mu_0 \sum_M \frac{\mathcal{M}_M^2}{\alpha_M^2} \dot{\gamma}_M^H \overline{\gamma_M^H} \right\}. \end{aligned} \quad (34)$$

Equation (34) is the main general result of the analysis of fields produced by uniformly moving sources in a straight beam pipe. It expresses the instantaneous Poynting flux crossing \mathcal{D} in terms of a mode sum over mode projections ρ_N of an axially-symmetric convective source with constant speed v and the longitudinal mode fields γ_N^E and γ_N^H given by (27). For sources with $v < c$ or sources that move off-axis such a summation must be performed numerically. However as noted above, for an ultra-relativistic source the fields are concentrated in the vicinity of the source and in the axially symmetric situation with bunches moving along the axis of the pipe one can effect a simplification. This permits a ready estimate of the power spectrum of the field pulse as

it traverses \mathcal{D} and it is this power spectrum that can, in principle, be detected by an advanced electro-optic detector and used to explore the distribution of charge in the pulse source.

We recall that in a cyclic machine with time-periodic fields of period T (such as a synchrotron) the fields associated with the sources can be expanded in a Fourier series:

$$\hat{\mathbf{e}}_n(z, r, \theta) = \frac{1}{T} \int_0^T \mathbf{e}(t, z, r, \theta) \exp(i\Omega t) dt \quad (35)$$

$$\hat{\mathbf{h}}_n(z, r, \theta) = \frac{1}{T} \int_0^T \mathbf{h}(t, z, r, \theta) \exp(i\Omega t) dt \quad (36)$$

where $\Omega = 2\pi/T$, and the mean (time-averaged) power crossing any area \mathcal{D} at z is

$$\langle \mathcal{P} \rangle (z) = \sum_{n=-\infty}^{\infty} \langle \mathcal{P}_n \rangle (z) \quad (37)$$

where

$$\langle \mathcal{P}_n \rangle (z) = \int_{\mathcal{D}} (\hat{\mathbf{e}}_n(z, r, \theta) \times \bar{\hat{\mathbf{h}}}_n(z, r, \theta)) \cdot \mathbf{e}_z r dr d\theta \quad (38)$$

However in a straight beam pipe the fields associated with the sources are not periodic in time. The sources are however localized in space so the total electromagnetic energy \mathcal{U} crossing any section \mathcal{D} at z is well-defined:

$$\mathcal{U}(z) = \int_{-\infty}^{\infty} \mathcal{P}(t, z) dt = \int_{-\infty}^{\infty} \left(\frac{d\mathcal{U}}{d\omega}(\omega, z) \right) d\omega \quad (39)$$

where

$$\frac{d\mathcal{U}}{d\omega}(\omega, z) = \int_{\mathcal{D}} \left(\hat{\mathbf{e}}(\omega, z, r, \theta) \times \bar{\hat{\mathbf{h}}}(\omega, z, r, \theta) \cdot \mathbf{e}_z \right) r dr d\theta \quad (40)$$

in terms of the Fourier transforms:

$$\hat{\mathbf{e}}(\omega, z, r, \theta) = \frac{1}{\sqrt{2\pi}} \int_{-\infty}^{\infty} \mathbf{e}(t, z, r, \theta) \exp(i\omega t) dt \quad (41)$$

$$\hat{\mathbf{h}}(\omega, z, r, \theta) = \frac{1}{\sqrt{2\pi}} \int_{-\infty}^{\infty} \mathbf{h}(t, z, r, \theta) \exp(i\omega t) dt \quad (42)$$

Clearly $\int_{\omega_1}^{\omega_2} \frac{d\mathcal{U}}{d\omega}(\omega, z) d\omega$ is the total electromagnetic energy crossing \mathcal{D} at the station z of the beam pipe in the wave band ω_1 to ω_2 and is experimentally accessible with suitable detector diagnostics. Measurement of the spectral content of such energy associated with charged electrons bunches of a few picoseconds in length is experimentally challenging. However new electro-optic techniques are being sought [6] that may use this content to deduce valuable information about the longitudinal charge distribution of such pulses.

In the ultra-relativistic limit the fields \mathbf{e} and \mathbf{h} have components that lie solely in the transverse sections of the pipe and are concentrated in space where the sources are concentrated. For an ultra-relativistic bunch

composed of an axially symmetric charge distribution with total charge Q moving along the beam pipe axis, one calculates from (40)

$$\frac{d\mathcal{U}}{d\omega} = K(a)|\hat{\rho}^{\parallel}(\omega, z)|^2 \quad (43)$$

where all the dependence of the pipe radius is contained in the constant

$$K(a) = \frac{c}{\epsilon_0} Q^2 \sum_M \frac{|\int_{\mathcal{D}} \mathcal{R}(r) \Phi_M(r, \theta) r dr d\theta|^2}{|2\pi\beta_M \int_0^a J_0^2(\beta_M r) r dr|^2} \quad (44)$$

In this source symmetric situation the “shielding” role of the pipe boundary is different from that played by “shielding” on CSR in a synchrotron [4].

In general one expects the source to require a stochastic description since its origin is fundamentally stochastic. This requires the introduction of stochastic variables and their associated probability distribution in order to calculate the expectation values of $\frac{d\mathcal{U}}{d\omega}$. However it is of interest first to note the deterministic structure of $\frac{d\mathcal{U}}{d\omega}$ that arises from a well-defined finite train of \mathcal{N} charged ultra-relativistic pulses where each pulse has the same longitudinal profile f in ρ^{\parallel} . Denote the longitudinal charge distribution ρ^{\parallel} of such a train by F with

$$F(z - ct) = F_0 \sum_{j=1}^{\mathcal{N}} f(z - c(t - T_j)) \quad (45)$$

for some real constant F_0 .

If $\hat{f}(\omega)$ is the Fourier transform of $f(t)$ then the Fourier transform of $\sum_{j=1}^{\mathcal{N}} f(t + \tau_j)$ with respect to t is $\hat{f}(\omega) \sum_{j=1}^{\mathcal{N}} \exp(-i\omega\tau_j)$ and

$$|\hat{f}(\omega) \sum_{j=1}^{\mathcal{N}} \exp(-i\omega\tau_j)|^2 = |\hat{f}(\omega)|^2 \left(\mathcal{N} + 2 \sum_{j=1}^{\mathcal{N}} \sum_{k=1}^{\mathcal{N}} \cos \omega(\tau_k - \tau_j) \right) \quad (46)$$

Hence for a train of such equidistant pulses with spatial separations $cT_0 > 0$

$$\frac{d\mathcal{U}}{d\omega}(\omega) = K(a)F_0^2 |\hat{f}(\omega)|^2 \mathcal{L}(\omega) \quad (47)$$

where $\mathcal{L}(\omega) = \frac{1 - \cos(\omega T_0 \mathcal{N})}{1 - \cos(\omega T_0)}$ and $\frac{d\mathcal{U}}{d\omega}$ is independent of z .

The function \mathcal{L} is bounded ($0 \leq \mathcal{L}(\omega) \leq \mathcal{N}^2$) with maxima at $\omega = \omega_j \equiv \frac{2\pi j}{T_0}$ but the detailed behaviour of $\frac{d\mathcal{U}}{d\omega}(\omega)$ depends on the single pulse structure defined by f . Thus if

$$f(z - c(t - T_j)) = \exp\left(-\left(\frac{z - c(t - T_j)}{\sigma_z}\right)^2\right) \quad (48)$$

describes the structure of the j -th pulse in the train with $T_j = j T_0$ one finds

$$\frac{d\mathcal{U}}{d\omega}(\omega) = K(a)F_0^2 \frac{\pi\sigma_z^2}{c^2} \mathcal{W}(\omega) \quad (49)$$

where

$$\mathcal{W}(\omega) = \exp\left(-\left(\frac{\omega\sigma_z}{\sqrt{2}c}\right)^2\right) \frac{1 - \cos(\omega T_0 \mathcal{N})}{1 - \cos(\omega T_0)} \quad (50)$$

The modulation of \mathcal{L} by $|\hat{f}|^2$ means that the maxima of $\mathcal{L} |\hat{f}|^2$ are shifted from $\omega = \omega_j$. For typical charged bunches described by the above Gaussian form for f the shift is unlikely to be experimentally detectable. However the points where $\omega = \omega_j$ determine the first order contact points of the curve $\frac{d\mathcal{M}}{d\omega}(\omega)$ with the envelope curve

$$\mathcal{E}^+(\omega) \equiv K(a)F_0^2 |\hat{f}|^2(\omega)\mathcal{N}^2 \quad (51)$$

i.e.

$$\lim_{\omega \rightarrow \omega_j} \left(\frac{\mathcal{E}^+(\omega)}{\frac{d\mathcal{M}}{d\omega}(\omega)} \right) = 1 \quad (52)$$

$$\lim_{\omega \rightarrow \omega_j} \left(\frac{(\mathcal{E}^+)'(\omega)}{\left(\frac{d\mathcal{M}}{d\omega}\right)'(\omega)} \right) = 1 \quad (53)$$

The general features of the spectrum of $\frac{d\mathcal{M}}{d\omega}$ for the choice of Gaussian f_j are sketched in figure 1. It should be stressed that the electromagnetic fields generated by the non-stochastic source under consideration are fully “coherent”. The maxima in $\frac{d\mathcal{M}}{d\omega}$ are produced by constructive interference of the fields associated with the regular structure in the train that is maintained during its ultra-relativistic motion. The spacing of adjacent maxima of $\frac{d\mathcal{M}}{d\omega}(\omega)$ produced by typical ultra-relativistic bunches in an accelerator differ imperceptibly from the spacing $\frac{2\pi}{T_0}$ of adjacent points where $\frac{d\mathcal{M}}{d\omega}$ is tangent to \mathcal{E}^+ . Thus the longitudinal spatial separation cT_0 of the maxima in this idealized bunch containing a structure with \mathcal{N} equidistant peaks is immediately visible in the electromagnetic energy spectrum.

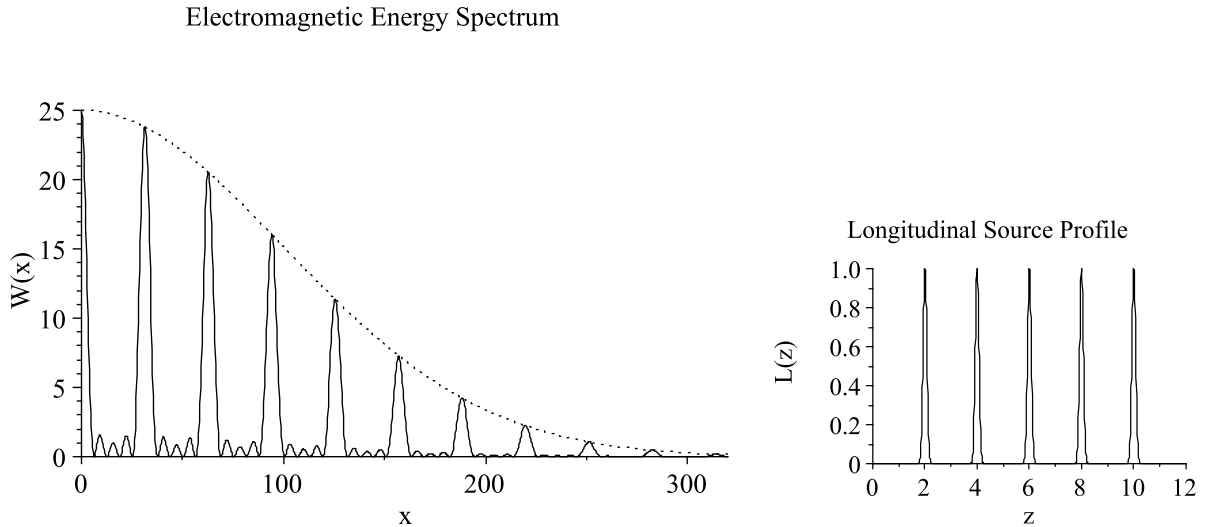


Figure 1: The rescaled electromagnetic energy spectrum with $x = T_0 \mathcal{N} \omega$:

$W(x) = \mathcal{W}\left(\frac{x}{T_0 \mathcal{N}}\right)$ associated with the longitudinal source profile

$L(z) \equiv \frac{F(z)}{F_0} = \sum_{j=1}^{\mathcal{N}} \exp\left(-\left(\frac{z - c_j T_0}{\sigma_z}\right)^2\right)$. For purposes of visualization $\sigma_z = \frac{1}{20}cT_0$, $\mathcal{N} = 5$, $T_0 = 1$, $c = 1$.

The upper dotted curve denotes the envelope $\frac{\mathcal{E}^+(x)}{(F_0^2 K(a))}$.

4 Stochastic Effects

To see the effects of randomization on these interference maxima a simple stochastic model of a charged bunch containing \mathcal{N} identifiable random variables will be adopted. Instead of fixing the separation of the \mathcal{N} peaks in ρ^{\parallel} they will be distributed according to some probability measure $P^{\mathcal{N}}$. We choose as random variables $T_1, T_2, \dots, T_{\mathcal{N}}$ and assume that

$$P^{\mathcal{N}}(T_1, T_2, \dots, T_{\mathcal{N}}) = \prod_{j=1}^{\mathcal{N}} P(T_j) \quad (54)$$

where $P(T)$ is a probability distribution for a single random variable T . The expectation value of any function \mathcal{O} of $T_1, T_2, \dots, T_{\mathcal{N}}$ will be denoted $E_{P^{\mathcal{N}}}(\mathcal{O})$ where

$$E_{P^{\mathcal{N}}}(\mathcal{O}) = \int_{R^{\mathcal{N}}} \mathcal{O}(T_1, T_2, \dots, T_{\mathcal{N}}) P^{\mathcal{N}}(T_1, T_2, \dots, T_{\mathcal{N}}) dT_1 dT_2 \dots dT_{\mathcal{N}} \quad (55)$$

In particular it follows from (46) that the expectation value of the spectral energy distribution is

$$E_{P^{\mathcal{N}}}\left(\frac{d\mathcal{U}}{d\omega}(\omega)\right) = K(a)F_0^2|\hat{f}|^2(\omega) E_{P^{\mathcal{N}}}(\mathcal{L}(\omega)) \quad (56)$$

where

$$E_{P^{\mathcal{N}}}(\mathcal{L}(\omega)) = \mathcal{N} + (\mathcal{N}^2 - \mathcal{N}) \left| \int_{-\infty}^{\infty} P(T) e^{i\omega T} dT \right|^2 \quad (57)$$

The magnitude of $(\mathcal{N}^2 - \mathcal{N})$ times the modulus squared of the Fourier transform of $P(T)$ in this expression relative to \mathcal{N} determines the nature of the expectation value of the spectral energy as a function of ω . This expectation value is now bounded above *and below* by two distinct envelopes that vary with ω . Within these envelopes one may in general classify local maxima as major and minor (see figure 3). The width of the first local dominant maxima in the ω spectrum of the expectation value is directly related to the overall scale of the spatial size of the bunch source as determined by the probability distribution $P(T)$ while the separation between adjacent local major maxima in $\frac{d\mathcal{U}}{d\omega}$ is determined by the structure of $P(T)$. These features are illustrated below where one notes that the bounding envelopes have single maxima at $\omega = 0$ in the ratio $\mathcal{N}^2 : \mathcal{N}$. For large \mathcal{N} this is then close to the ratio of the first few ratios of (local maxima : local minima) of $\frac{d\mathcal{U}}{d\omega}$. Following tradition it is natural to refer to fields that contribute to the first few major local maxima of $\frac{d\mathcal{U}}{d\omega}$ as exhibiting ‘‘stochastic coherence’’. The relation between the non-zero frequency at which the first local minimum of $\frac{d\mathcal{U}}{d\omega}$ occurs (or the frequency beyond which $\frac{d\mathcal{U}}{d\omega}$ lies close to the lower bounding envelope) and the spatial distribution of charge in ρ^{\parallel} is a stochastic one depending on the structure of $P(T)$. These general features are illustrated as follows.

- If \mathcal{N} identical pulses in ρ^{\parallel} , each with the above longitudinal Gaussian profile f , are, for some constant Γ , independently distributed according to $P^{\mathcal{N}}$ with:

$$P(T) = \frac{1}{\Gamma} \quad \text{for} \quad -\frac{\Gamma}{2} \leq T \leq \frac{\Gamma}{2} \quad (58)$$

and zero elsewhere then

$$E_{P\mathcal{N}} \left(\frac{d\mathcal{U}}{d\omega}(\omega) \right) = K(a)F_0^2 |\hat{f}|^2(\omega) \left(\mathcal{N} + (\mathcal{N}^2 - \mathcal{N}) \left(\frac{\sin(\omega\Gamma/2)}{\omega\Gamma/2} \right)^2 \right). \quad (59)$$

The bounding envelopes (see figure 2) are the curves $\mathcal{E}^-(\omega) = K(a)F_0^2 \mathcal{N} |\hat{f}|^2(\omega)$ and $\mathcal{E}^+(\omega) = K(a)F_0^2 \mathcal{N}^2 |\hat{f}|^2(\omega)$:

$$\mathcal{E}^-(\omega) \leq E_{P\mathcal{N}} \left(\frac{d\mathcal{U}}{d\omega}(\omega) \right) \leq \mathcal{E}^+(\omega) \quad (60)$$

It is natural to designate the Fourier components of fields as “stochastically incoherent” if they contribute to the expectation $E_{P\mathcal{N}} \left(\frac{d\mathcal{U}}{d\omega}(\omega) \right)$ in the vicinity of the lower bounding envelope $\mathcal{E}^-(\omega)$. This expectation value first touches $\mathcal{E}^-(\omega)$ at approximately $\omega = \frac{2\pi}{\Gamma}$ and Γ determines the average spatial length of ρ^\parallel .

Electromagnetic Energy Spectrum

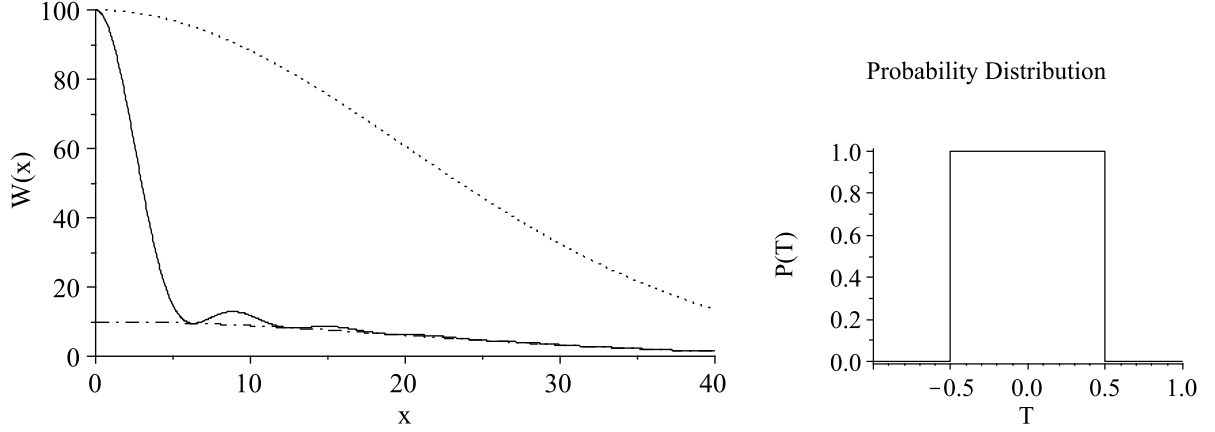


Figure 2: The rescaled electromagnetic energy spectrum with $x = \Gamma\omega$: $W(x) = E_{P\mathcal{N}} \left(\frac{d\mathcal{U}}{d\omega} \left(\frac{x}{\Gamma} \right) \right) / (F_0^2 K(a))$ associated with the longitudinal probability distribution $P(T) = 1/\Gamma$ for $-\Gamma/2 \leq T \leq \Gamma/2$. For purposes of visualization $\sigma_z = \frac{1}{20}c\Gamma$, $\Gamma = 1$, $c = 1$, $\mathcal{N} = 10$. The upper dotted curve denotes the envelope $\frac{\mathcal{E}^+(x)}{(F_0^2 K(a))}$ and the lower one the envelope $\frac{\mathcal{E}^-(x)}{(F_0^2 K(a))}$.

- If, for some integer n and constant κ , \mathcal{N} identical pulses in ρ^\parallel , each with the above longitudinal Gaussian profile f , are independently distributed according to $P^\mathcal{N}$ with:

$$P(T) = \frac{1}{(2n+1)\kappa\sqrt{\pi}} \sum_{j=-n}^n \exp \left(- \left(\frac{T - j\tau}{\kappa} \right)^2 \right) \quad \text{for } -\infty \leq T \leq \infty \quad (61)$$

then

$$E_{P\mathcal{N}} \left(\frac{d\mathcal{U}}{d\omega}(\omega) \right) = K(a)F_0^2 |\hat{f}|^2(\omega) \left(\mathcal{N} + (\mathcal{N}^2 - \mathcal{N}) \frac{1}{(2n+1)^2} \exp \left(- \left(\frac{\omega\kappa}{\sqrt{2}} \right)^2 \right) \frac{1 - \cos(\omega\tau(2n+1))}{1 - \cos(\omega\tau)} \right) \quad (62)$$

Such a distribution $P(T)$ offers a means to model the electromagnetic energy associated with a bunch containing \mathcal{N} constituents with $2n+1$ micro-bunches [11] distributed stochastically among them according

to equally spaced Gaussian distributions with parameters κ and τ .

In this case the bounding envelopes (see figure 3) are the curves

$$\mathcal{E}^-(\omega) = K(a)F_0^2 \mathcal{N} |\hat{f}|^2(\omega), \quad (63)$$

$$\mathcal{E}^+(\omega) = K(a)F_0^2 |\hat{f}|^2(\omega) \left(\mathcal{N} - (\mathcal{N}^2 - \mathcal{N}) \exp\left(-\frac{\omega^2 \kappa^2}{2}\right) \right) \quad (64)$$

and

$$\mathcal{E}^-(\omega) \leq E_{P\mathcal{N}} \left(\frac{d\mathcal{U}}{d\omega}(\omega) \right) \leq \mathcal{E}^+(\omega) \quad (65)$$

For $\omega \neq 0$ the envelope $\mathcal{E}^-(\omega)$ here lies below the envelope $\mathcal{E}^+(\omega)$ for the previous distribution in figure 2. Hence the overall effect of the micro-structure introduced in this $P(T)$ is to suppress the magnitude of the $j > 0$ local major maxima near $\omega = \frac{2\pi j}{\tau}$ in the expectation values of $\frac{d\mathcal{U}}{d\omega}$.

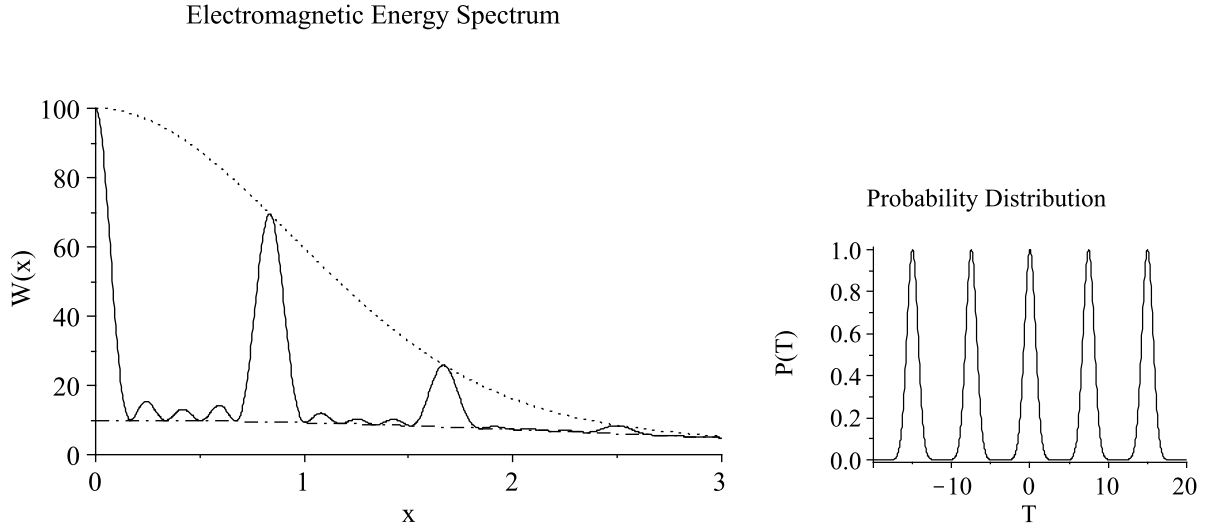


Figure 3: The rescaled electromagnetic energy spectrum with $x = \kappa\omega$: $W(x) = E_{P\mathcal{N}} \left(\frac{d\mathcal{U}}{d\omega} \left(\frac{x}{\kappa} \right) \right) / (F_0^2 K(a))$ associated with the probability distribution

$$P(T) = ((2n+1)\kappa\sqrt{\pi})^{-1} \sum_{j=-n}^n \exp(-(T-j\tau)^2 \kappa^{-2}).$$

For purposes of visualization $\sigma_z = \frac{2}{5}c\kappa$, $\tau = 30\kappa(n-1)^{-1}$, $\mathcal{N} = 10$, $n = 2$, $\kappa = 1$, $c = 1$. The upper dotted curve denotes the envelope $\frac{\mathcal{E}^+(x)}{(F_0^2 K(a))}$ and the lower one the envelope $\frac{\mathcal{E}^-(x)}{(F_0^2 K(a))}$.

5 Conclusions

Electromagnetic energy spectra associated with distributions of charge in uniform ultra-relativistic motion in a perfectly conducting straight cylindrical beam pipe have been calculated based on a number of detailed models. The electromagnetic fields have been calculated ab-initio by solving analytically the initial-boundary value problem for Maxwell's equations in the beam pipe. The effects of the pipe geometry and the source proper charge distribution on the field structure have been explored for different stochastic models. The salient features of the spectral distributions have been compared with analogous properties in a cyclic machine. Further aspects of such dynamically enhanced field effects can be found in [12]. We feel that these results have relevance to

current experimental techniques for measuring the longitudinal charge distribution of ultra-relativistic electron bunches with micro-structure using electro-optic techniques from observation of their associated electromagnetic energy spectra.

Acknowledgments

The authors are grateful to D. A. Burton, A. Cairns, S. P. Jamison and A. Wolski for valuable discussions and to the Cockcroft Institute, STFC and EPSRC for financial support for this research.

References

- [1] J Schwinger, *On the Classical Radiation of Accelerated Electrons*, Phys. Rev. **75** 1912, (1949).
- [2] J Schwinger, *Electron Radiation in High Energy Accelerators*, Phys. Rev. **70** 798, (1946).
- [3] A Hofmann, *The Physics of Synchrotron Radiation*, (Cambridge University Press, 2004).
- [4] J S Nodvick, D S Saxon, *Suppression of Coherent Radiation by Electrons in a Synchrotron*, Phys. Rev. **96** 180, (1954).
- [5] E L Saldin, E A Schneidmiller, M V Yurkov *Coherent Radiation of an Electron Bunch Moving in an Arc of a Circle*, Nuclear Instruments and Methods in Physics Research A **398** 373-394, (1997).
- [6] S P Jamison, et al, *Femtosecond Resolution Electron Bunch Profile Measurements*, Proceedings of EPAC 2006 Edinburgh Scotland 915-919, (2006).
- [7] D S Jones, *The Theory of Electromagnetism*, (Pergamon Press, 1964).
- [8] R W Tucker, *On the Effects of Geometry on Guided Electromagnetic Waves*, Theoret. Appl. Mech. **34** 1-49, (2007).
- [9] S Goto, R W Tucker, *Electromagnetic Fields Produced by Moving Sources in a Curved Beam Pipe*, J.Math Phys. **50** 063510, (2009).
- [10] M A Pinsky, *Partial Differential Equations and Boundary-Value Problems with Applications*, (McGraw-Hill, Inc., 1991).
- [11] G Stupakov, S Heifets, *Beam Instability and Microbunching Due to Coherent Synchrotron Radiation*, Phys. Rev. ST Accel. Beams **5** 054402, (2002).
- [12] A C Hale, *Aspects of Dynamically Enhanced Electromagnetic Fields from Charged Relativistic Sources in a Beam Pipe*, (PhD Thesis, Lancaster University, 2008).